# Supplemental Figure 1

## High magnification images supplements Figure 1

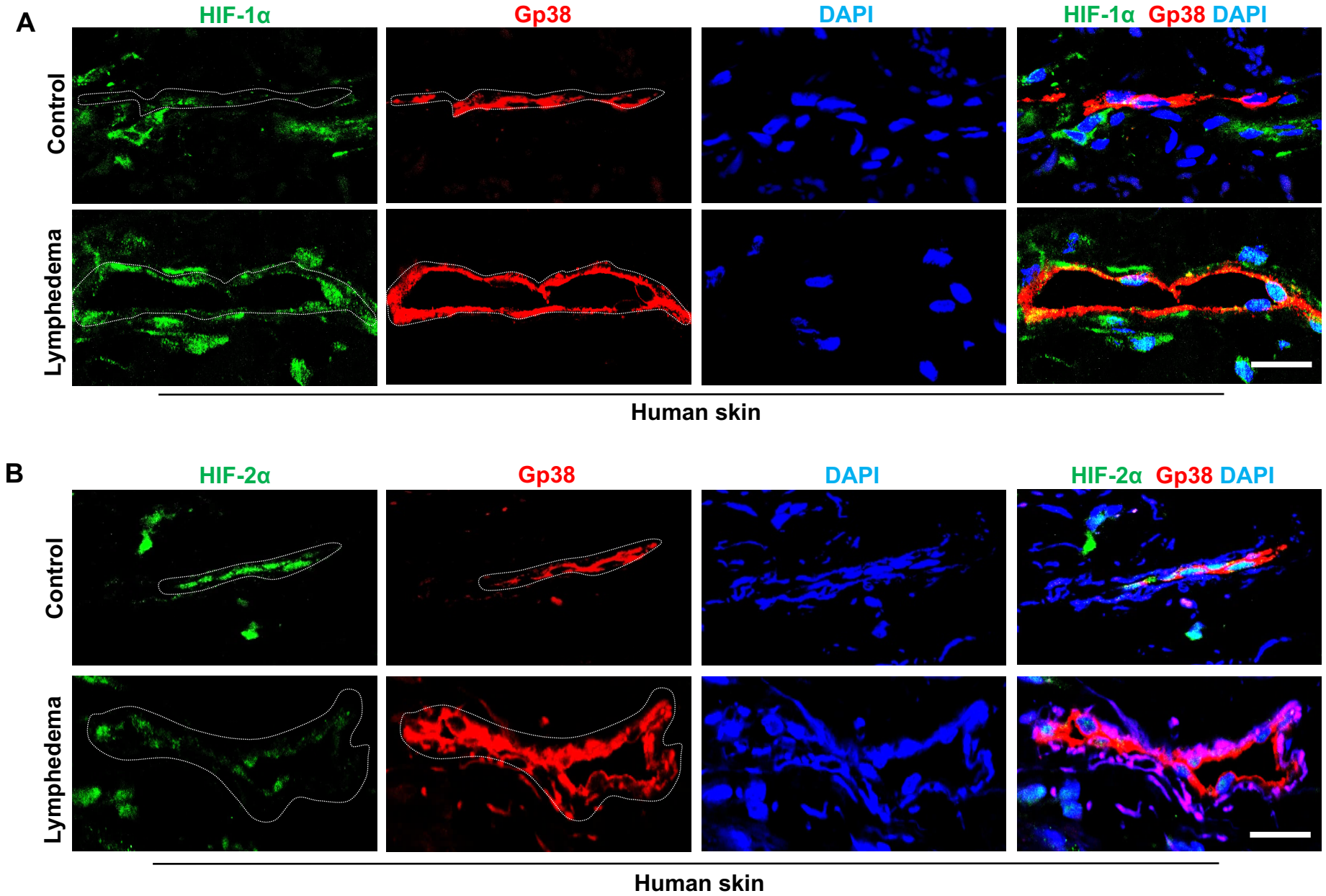

# Supplemental Figure 2

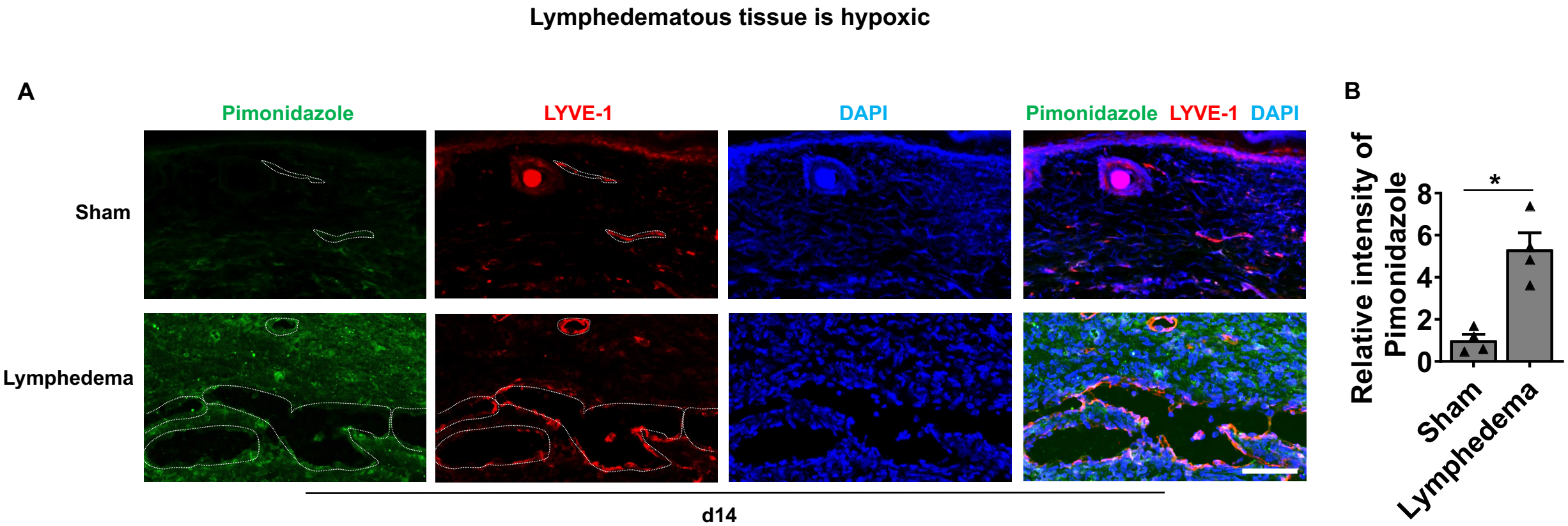

# Supplemental Figure 3

## Lymphatic specific reporter or *Hif* knockout or overexpression mice and the timeline for lymphedema study

A

| Symbol | Genotype | Purpose |
|---|---|---|
| Lymphatic reporter | *Prox-1-CreERT2*, LSL*tdTomato* | LEC specific tdTomato expression |
| *Hif2α* LECKO | *Prox-1-CreERT2, Hif2α(fl/fl)* | LEC specific *Hif2α* knockout |
| *Hif2α* LECOE | *Prox-1-CreERT2, LSLHif2α* | LEC specific *Hif2α* overexpression |
| *Hif1α* LECKO | *Prox-1-CreERT2, Hif1α(fl/fl)* | LEC specific *Hif1α* knockout |

B

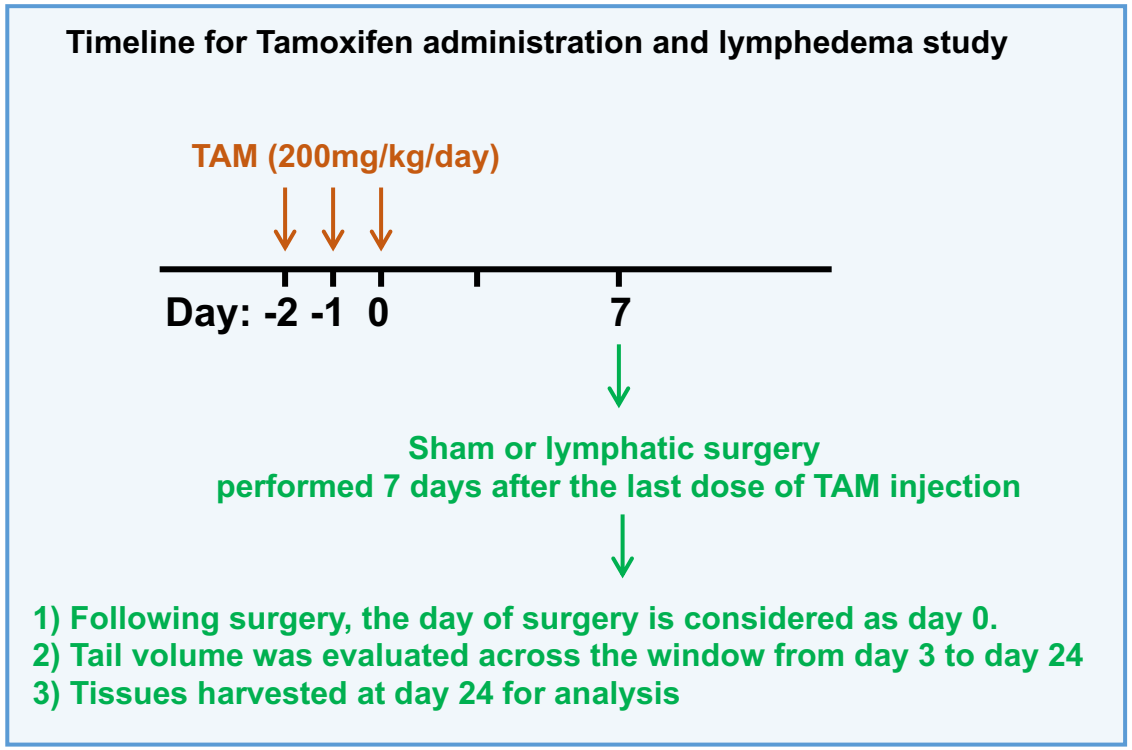

# Supplemental Figure 4

**No observable spontaneous, tamoxifen-independent, CreERT2-mediated tdTomato induction**

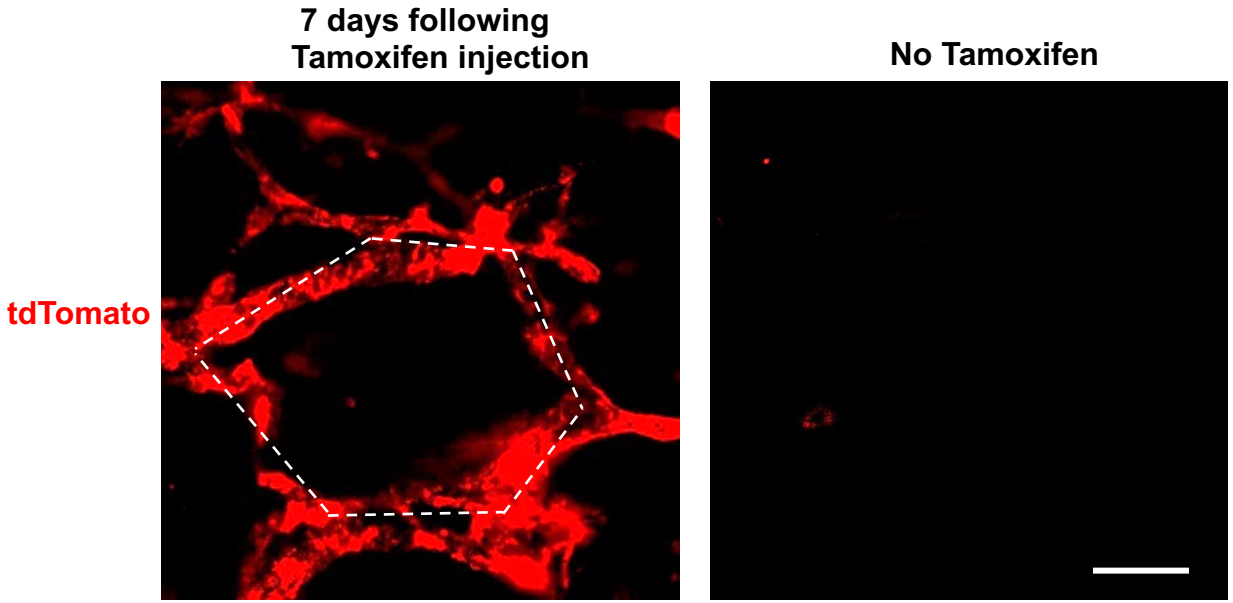

**Supplemental Figure 5**

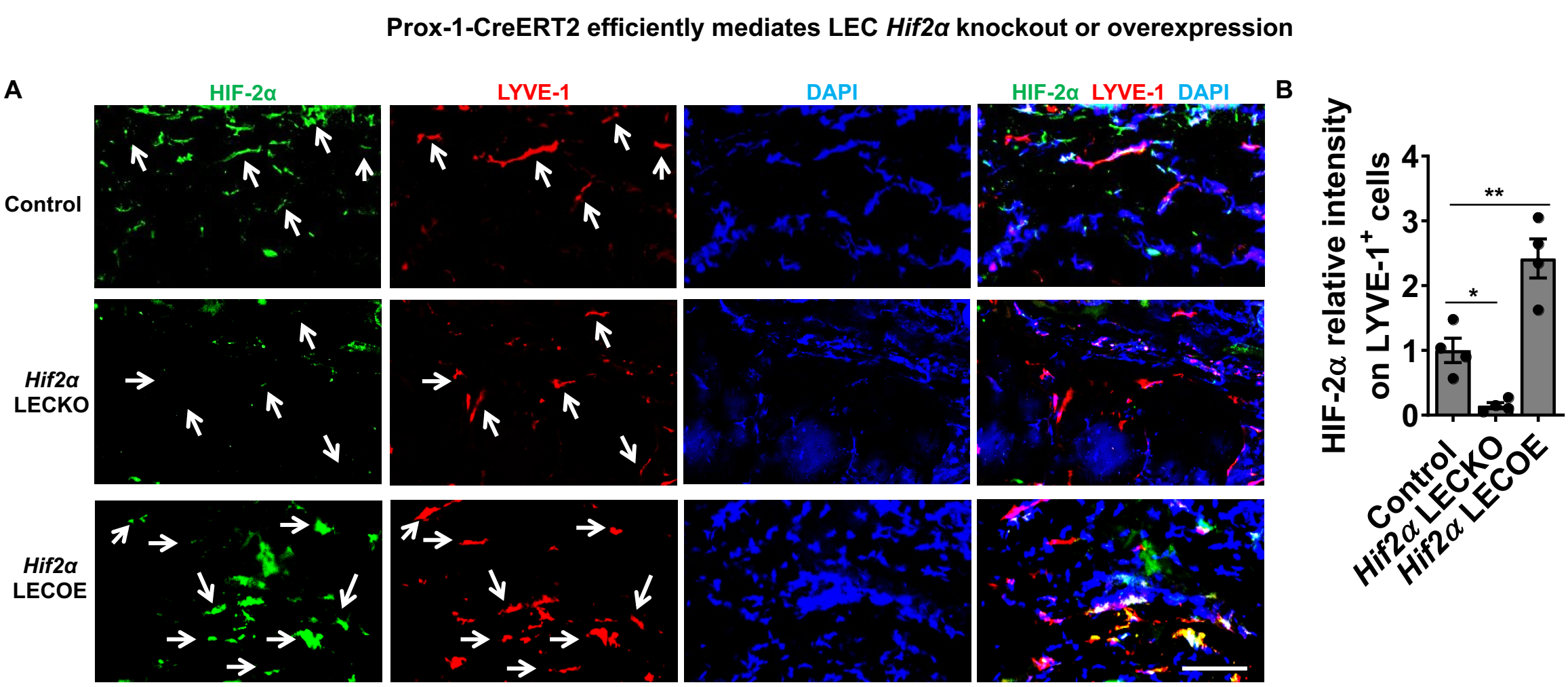

**Supplemental Figure 6**

## Prox-1-CreERT2 efficiently mediates LEC *Hif1α* knockout

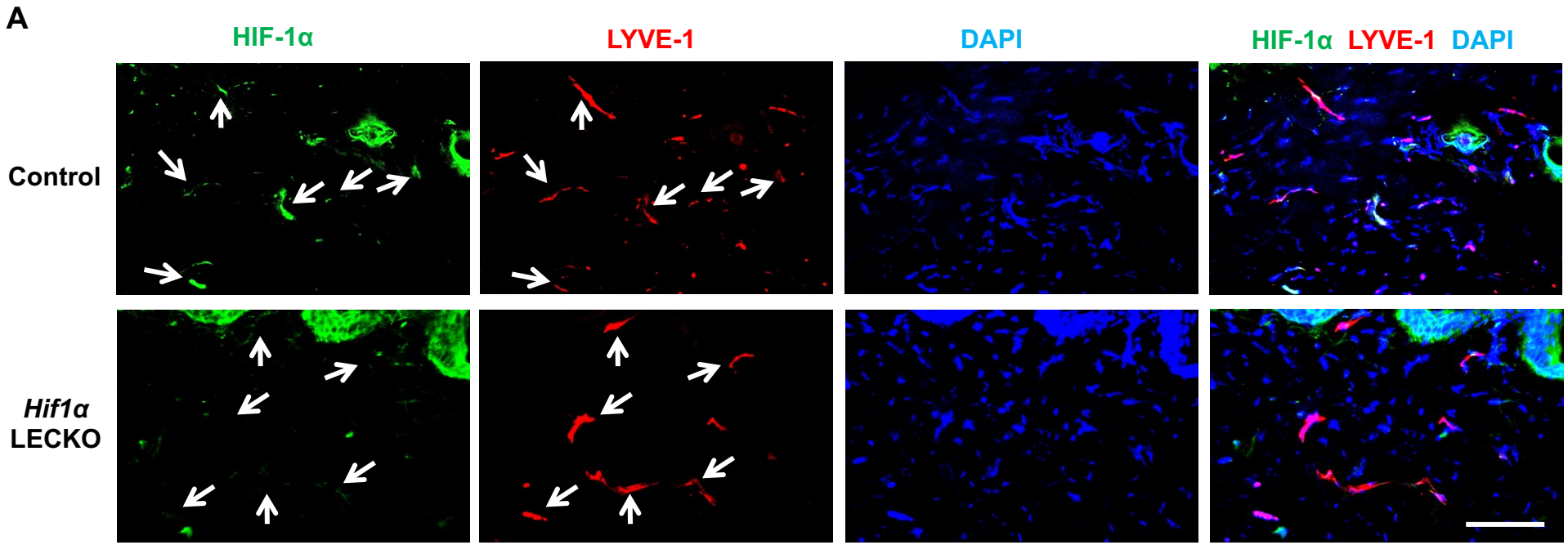


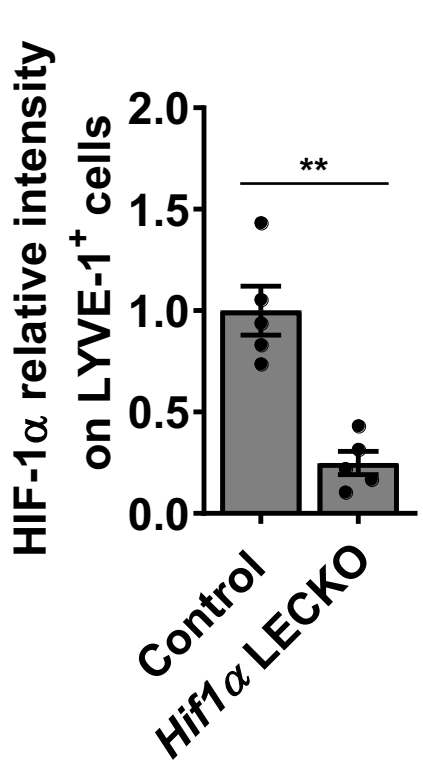

## Supplemental Figure 7

### Low LEC HIF-1α expression in lymphedematous skin of *Hif1α* LECKO mice

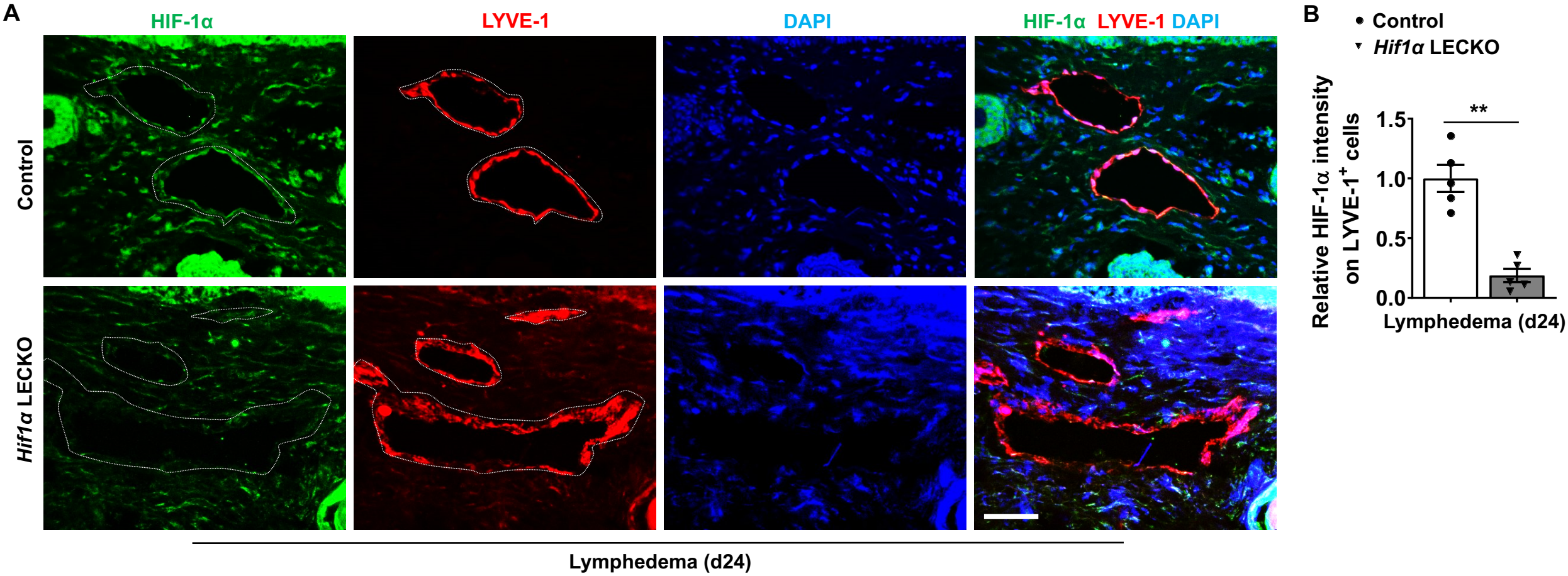

**Supplemental Figure 8**

**LEC *Hif1α* deletion causes an increased but non-sustained rise in mouse tail volume**

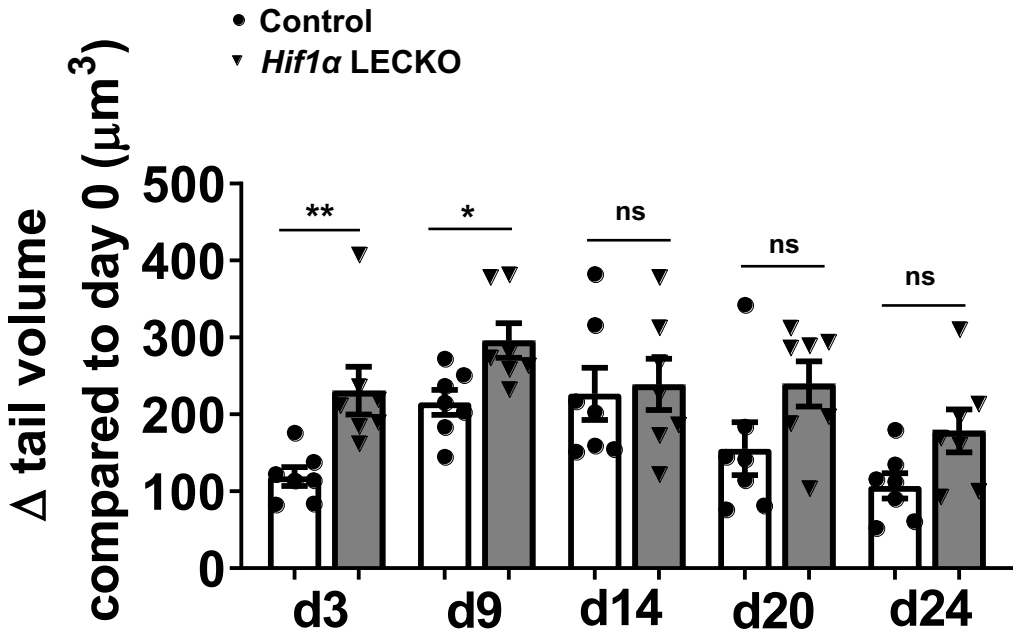

# Supplemental Figure 9

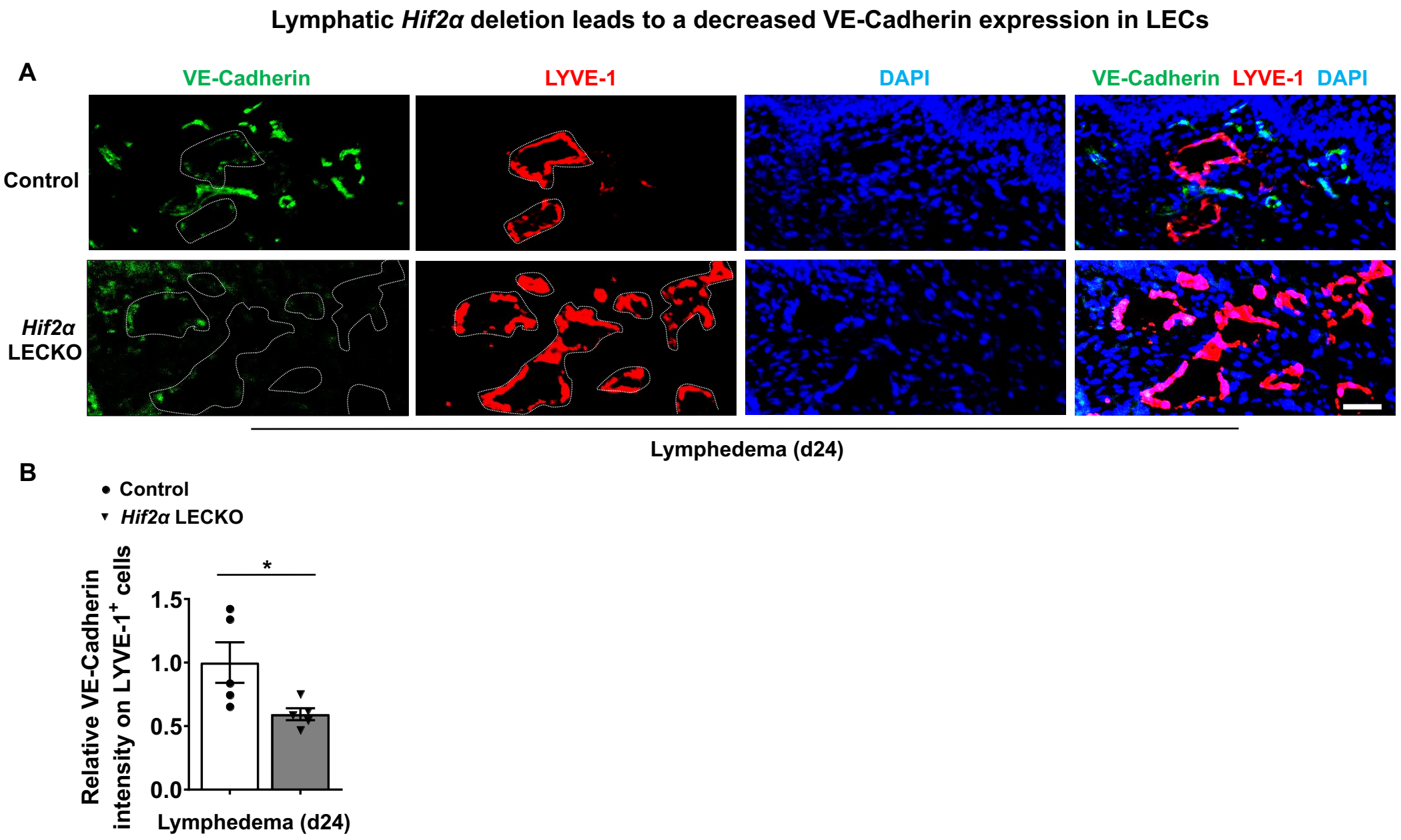

**Supplemental Figure 10**

## Myeloid cell *Hif2α* knockout caused transient worsening of tail swelling

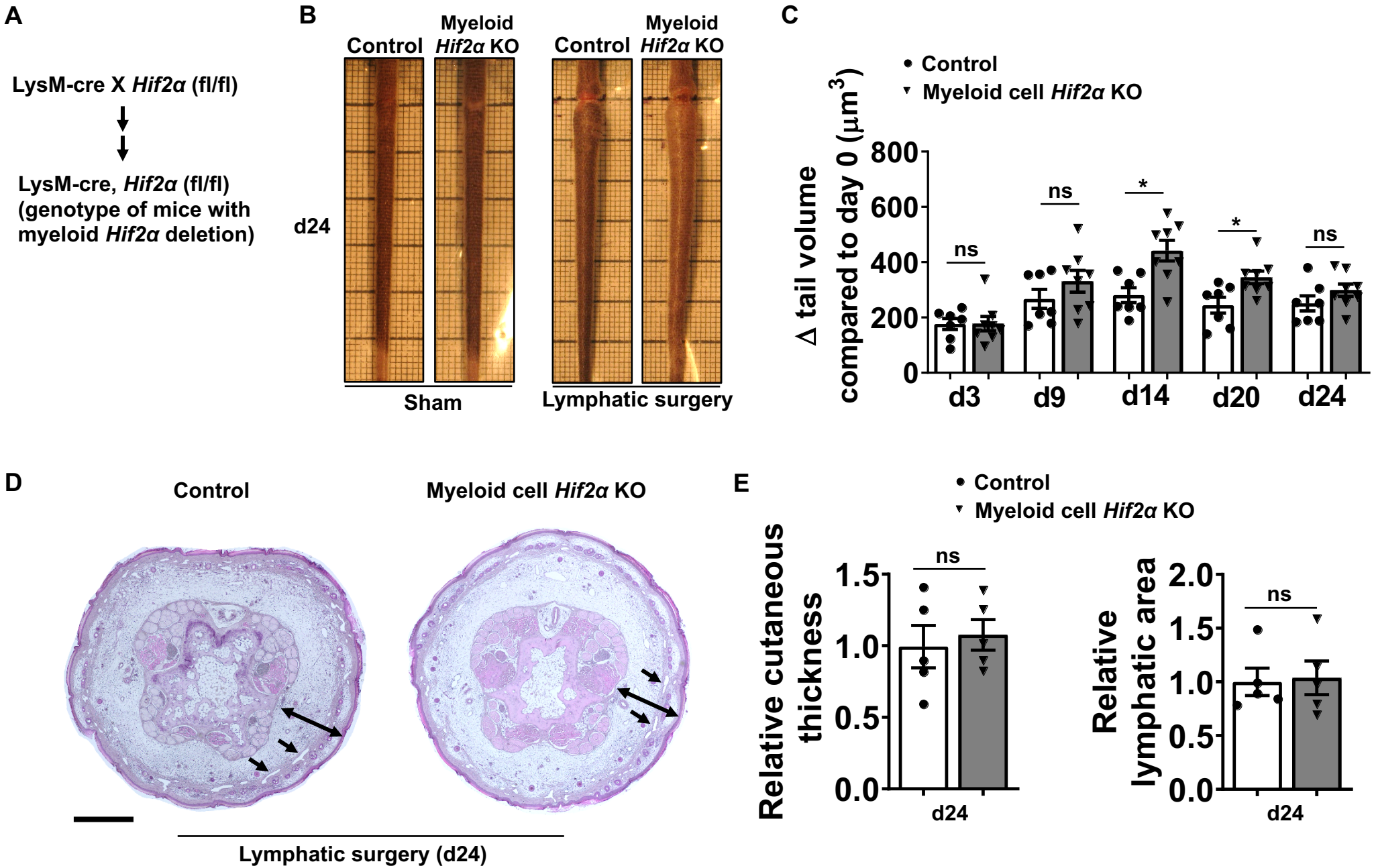

**Supplemental Figure 11**

## Prox-1-CreERT2 efficiently mediates LEC *Hif2α* knockout in embryo dorsal skin

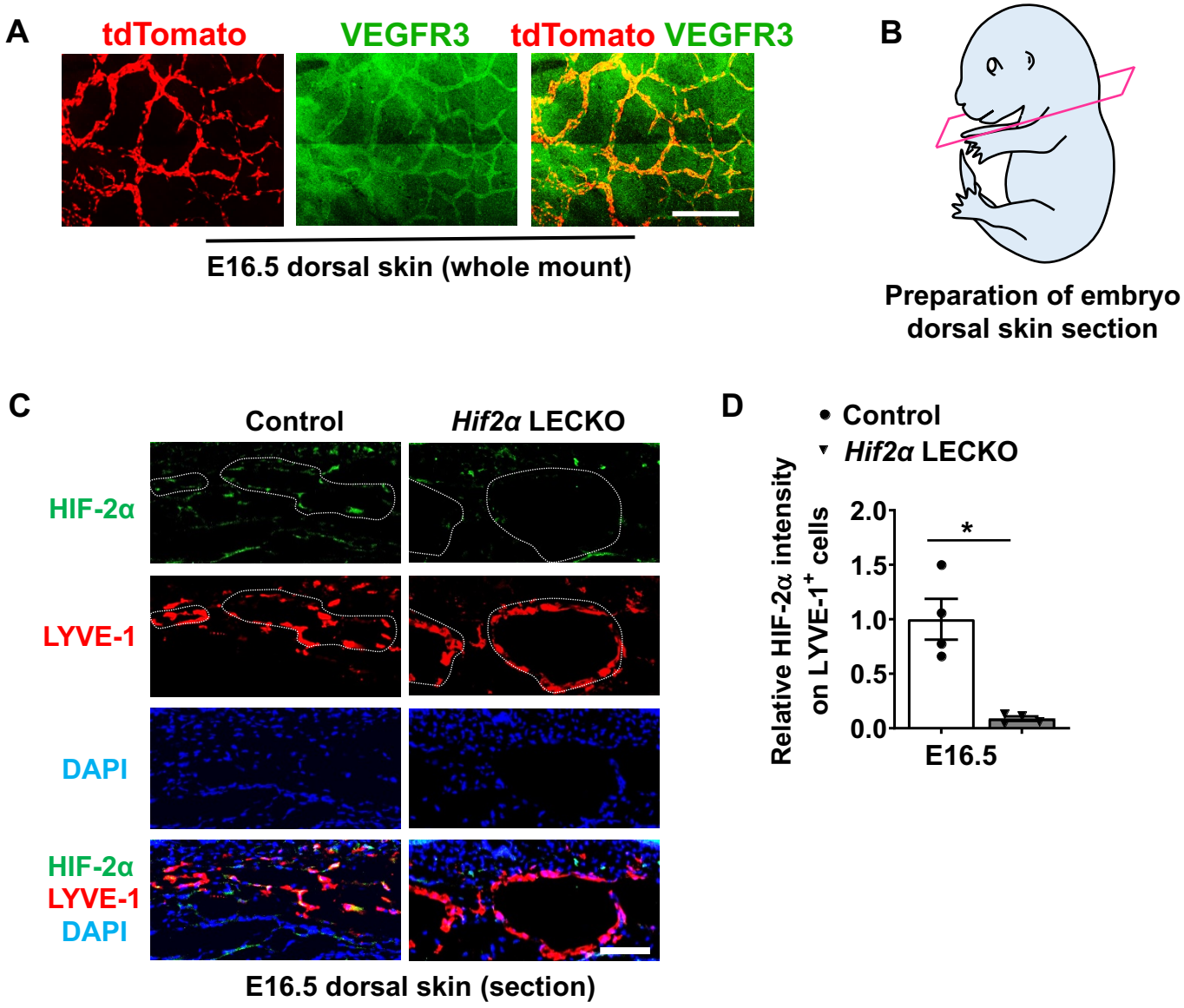

**Supplemental Figure 12**

## LEC *Hif2α* knockout causes abnormal tail and tracheal lymphatic remodeling

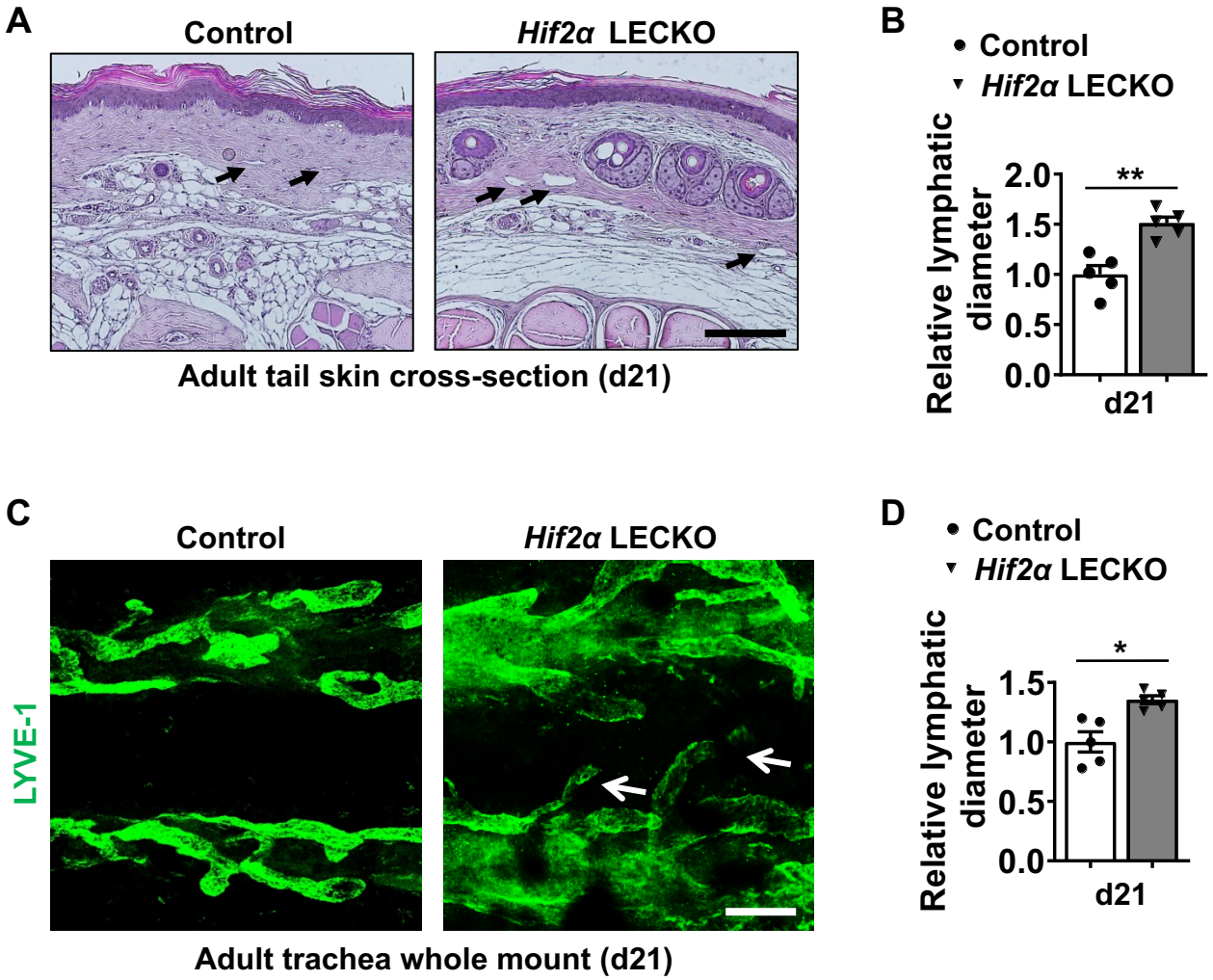

**Supplemental Figure 13**

## Decreased LEC TIE2 and p-TIE2 expression in the dorsal skin of E16.5 *Hif2α* LECKO embryos

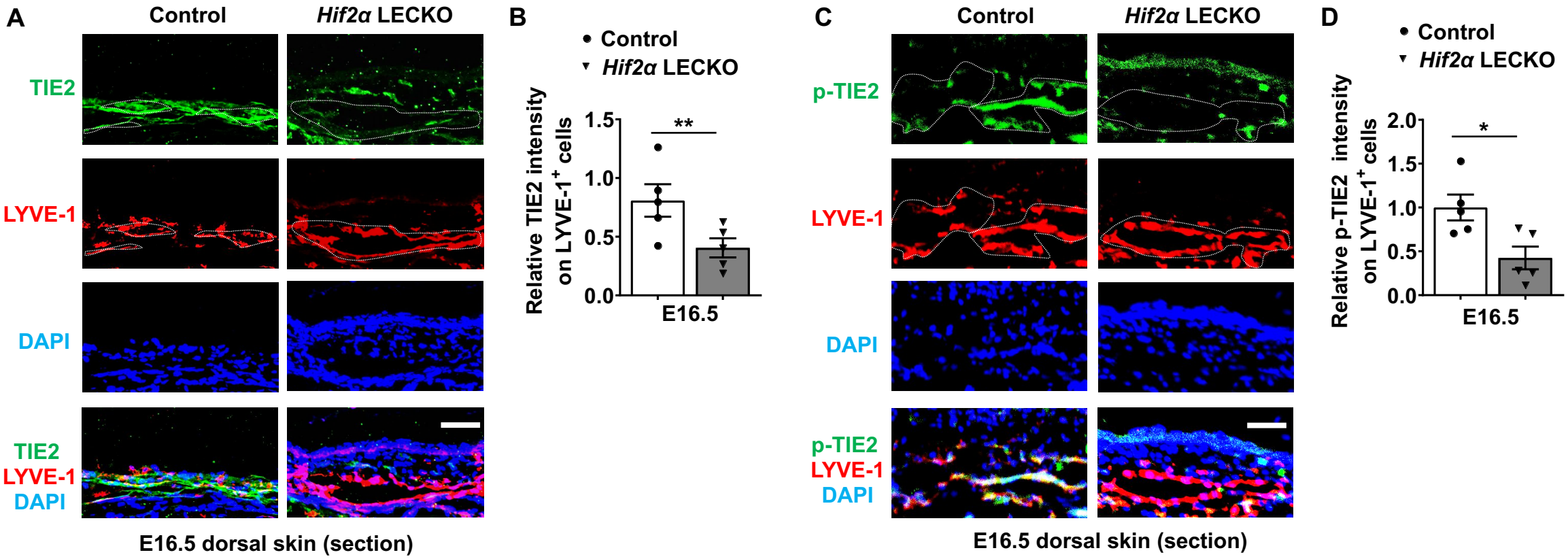

**Supplemental Figure 14**

**Ad*Angpt1,* but not Ad*Angpt2,* treatment attenuates tail swelling in WT mice subject to lymphatic surgery**

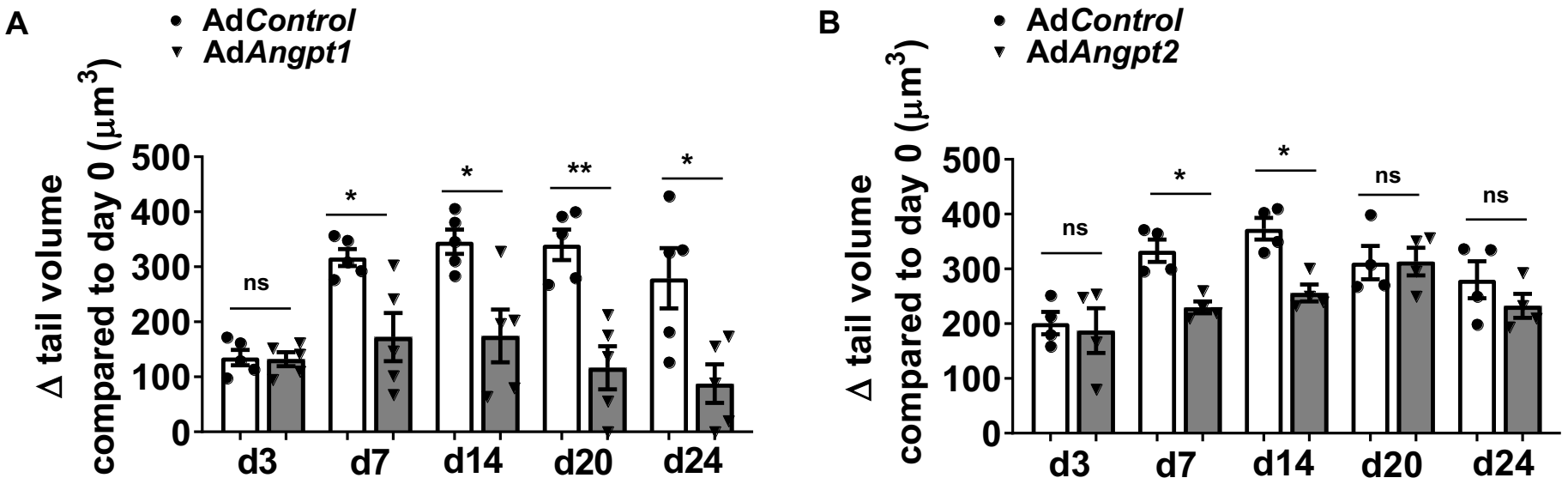

**Supplemental Figure 15**

## Sustained LEC HIF-2α expression in lymphedematous skin of *Hif2α* LECOE mice

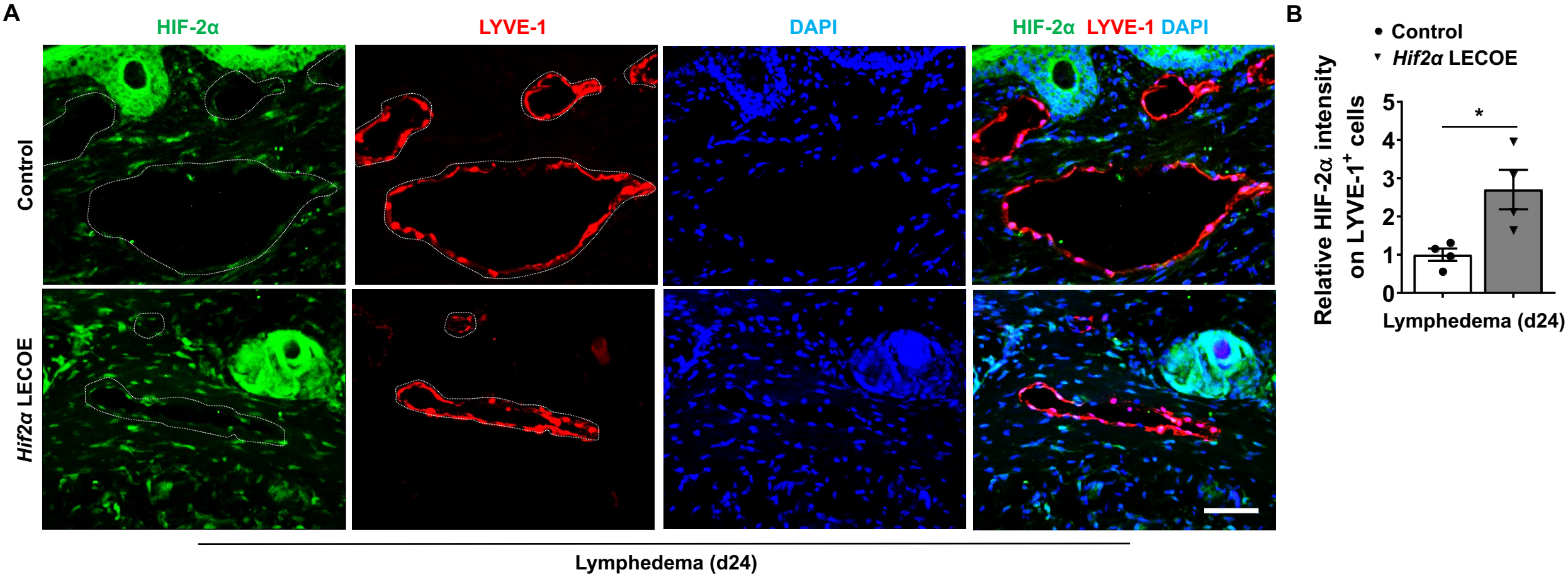

**Supplemental Figure 16**

## LEC *Hif2α* overexpression reduces tissue CD45$^{+}$ cell numbers following lymphatic surgery

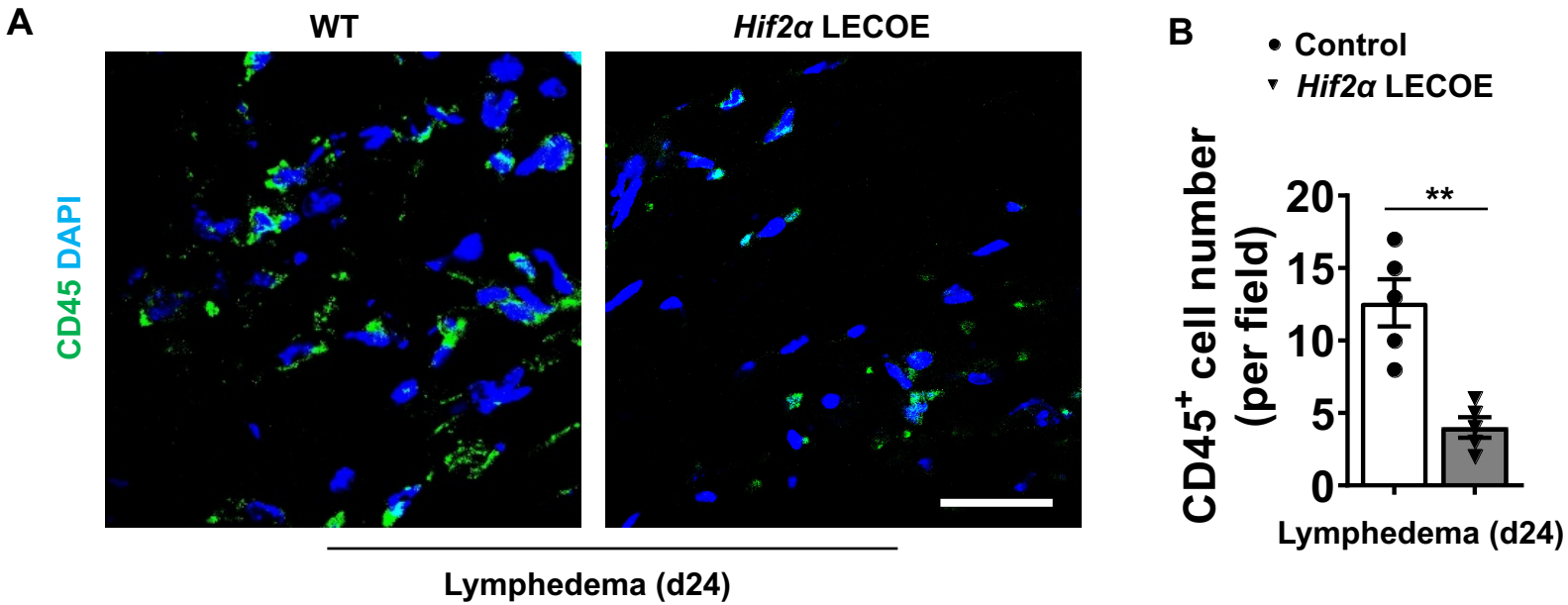

**Supplemental Figure 1. High magnification images supplements Figure 1.** (**A**) Immunofluorescence staining of HIF-1α (green) and Gp38 (red) in control and lymphedematous clinical samples. DAPI (blue) stains the nucleus. White dashed lines demarcate lymphatics. (**B**) Immunofluorescence staining of HIF-2α (green) and Gp38 (red) of human samples. DAPI (blue) stains the nucleus. White dashed lines demarcate lymphatics. Scale bars: 30 μm (**A** and **B**).

**Supplemental Figure 2. Lymphedematous tissue is hypoxic.** (**A**) Hypoxyprobe (pimonidazole) staining. Representative immunofluorescence staining images of LYVE-1 (red) and pimonidazole (green) of tails of mice subjected to sham or lymphatic surgery (d14). White dashed lines demarcate the lymphatics. DAPI (blue) stains the nucleus. (**B**) Quantification of pimonidazole intensity comparing the groups shown in **A** (n=4); data are presented as mean ± SEM; *P<0.05 by the Mann-Whitney test. n represents numbers of mice. Scale bar: 60 μm (**A**).

**Supplemental Figure 3. Lymphatic-specific transgenic mice and experimental timeline.** (**A**) Summary of tdTomato lymphatic reporter mice and LEC-specific *Hif* loss-of-function transgenic mice strains. (**B**) Schematics illustrating the timeline of tamoxifen (TAM)-induced gene modification for lymphedema study.

**Supplemental Figure 4. Negligible spontaneous, tamoxifen-independent, CreERT2-mediated tdTomato induction.** Whole-mount mouse skin images showing tdTomato fluorescence, which highlights typical mouse tail lymphatic vascular structure in tamoxifen-administered mice, but not in those that did not receive the same treatment. Dashed white lines outline the hexagonal lymphatic capillaries of the tail skin. Scale bar: 100 μm.

**Supplemental Figure 5. Prox-1-CreERT2 efficiently mediates LEC *Hif2α* knockout or overexpression.** (**A**) Representative immunofluorescence staining of HIF-2α (green) and LYVE-1 (red) of skin tissues harvested from control or *Hif2α* LECKO or *Hif2α* LECOE mice. DAPI (blue) stains nucleus. White arrows point to LYVE-1 expressing lymphatics. (**B**) Quantification of HIF-2α intensity comparing groups shown in **A** (n=4). Data are presented as mean ± SEM; *P<0.05; **P<0.01; by 1-way ANOVA followed by Tukey's multiple comparison test. n represents numbers of mice. Scale bar: 100 μm (**A**).

**Supplemental Figure 6. Prox-1-CreERT2 efficiently mediates LEC *Hif1α* knockout.** (**A**) Representative immunofluorescence staining of HIF-1α (green) and LYVE-1 (red) of skin tissues harvested from control or *Hif1α* LECKO mice. DAPI (blue) stains nucleus. White arrows point to LYVE-1 positive lymphatics. (**B**) Quantification of HIF-1α intensity comparing groups shown in **A** (n=5). Data are presented as mean ± SEM; **P<0.01; by the Mann-Whitney test. n represents numbers of mice. Scale bar: 100 μm (**A**).

**Supplemental Figure 7. Low LEC HIF-1α expression in lymphedematous skin of *Hif1α* LECKO mice.** (**A**) Representative immunofluorescence staining of HIF-1α (green) and LYVE-1 (red) of skin tissues harvested from control or *Hif1α* LECKO mice subjected to lymphatic surgery. DAPI (blue) stains nucleus. White dashed lines demarcate enlarged lymphatics. (**B**) Quantification of HIF-1α intensity comparing groups shown in **B** (n=5). Data are presented as mean ± SEM; **P<0.01; by the Mann-Whitney test. n represents numbers of mice. Scale bar: 60 μm (**A**).

**Supplemental Figure 8. LEC *Hif1α* deletion modestly aggravates tail volume increase following lymphatic surgery.** Serial tail volume measurements of control and *Hif1α* LECKO

mice with lymphatic surgery (n=7). Data are presented as mean ± SEM; ns, not significant; *P<0.05; **P<0.01; by the Mann-Whitney test. n represents numbers of mice.

**Supplemental Figure 9. Declined LEC VE-Cadherin expression in the skin of *Hif2α* LECKO mice subjected to lymphatic surgery compared to that of WT controls.** (**A**) Representative immunofluorescence staining of VE-Cadherin (green) and LYVE-1 (red) of skin tissues harvested from WT control or *Hif2α* LECKO mice subjected to lymphatic surgery. DAPI (blue) stains nucleus. White dashed lines demarcate enlarged lymphatics. (**B**) Quantification of VE-Cadherin intensity comparing groups shown in **B** (n=5). Data are presented as mean ± SEM; *P<0.01; by the Mann-Whitney test. n represents numbers of mice. Scale bar: 60 μm (**A**).

**Supplemental Figure 10. Myeloid cell *Hif2α* deletion causes transient worsening of tail swelling.** (**A**) Brief summary of breeding strategy for creating myeloid specific *Hif2α* knockout by cross LysM-Cre mice with *Hif2α* (fl/fl) mice. (**B**) Representative images of WT or myeloid *Hif2α* KO tail 24 days following sham or lymphatic surgery. (**C**) Serial tail volume measurement of WT and myeloid *Hif2α* KO mice with lymphatic surgery (n=7-8). (**D**) Representative H&E staining of tails of WT or myeloid *Hif2α* KO mice with lymphatic surgery. Black arrows point to dilated lymphatics, double-headed black arrows illustrate the cutaneous layer thickness. (**E**) Quantification of cutaneous thickness and lymphatic area comparing groups shown in **D** (n=5). **C** and **E**, data are presented as mean ± SEM; ns, not significant; *P<0.05; the Mann-Whitney test. n represents numbers of mice. Scale bar: 500 μm (**D**).

**Supplemental Figure 11. Prox-1-CreERT2 efficiently mediates LEC *Hif2α* knockout in the dorsal skin of the embryos.** (**A**) Representative whole-mount immunofluorescence images tdTomato (red) and VEGFR3 (green) of skin tissues harvested from control or *Hif2α* LECKO E16.5 embryos. DAPI (blue) stains nucleus. (**B**) A schematic diagram showing preparation of tissue sections of E16.5 embryo for immunofluorescence staining. (**C**) Representative immunofluorescence staining of HIF-2α (green) and LYVE-1 (red) of dorsal skin of the cervical area from WT control or *Hif2α* LECKO embryos. DAPI (blue) stains nucleus. White dashed lines demarcate lymphatics. (**D**) Quantification of HIF-2α intensity comparing groups shown in **C** (n=4). Data are presented as mean ± SEM; *P<0.05; by the Mann-Whitney test. n represents numbers of embryos from 3 litters. Scale bars: 200 μm (**A**) and 60 μm (**C**)

**Supplemental Figure 12. LEC *Hif2a* deficiency causes abnormal tail and tracheal lymphatic remodeling.** (**A**) Representative H&E images of control or *Hif2α* LECKO tail 21 days after tamoxifen administration, black arrows point to lymphatic vessels. (**B**) Quantification of lymphatic diameter comparing the groups shown in **A** (n=5). (**C**) Representative whole mount immunofluorescence staining of LYVE-1 (green) of tracheas from control or *Hif2α* LECKO mice 21 days after gene deletion. White arrows point to lymphatics sprouting into the cartilaginous area. (**D**) Quantification of lymphatic diameter comparing the groups shown in **C** (n=5). **B** and **D**, data are presented as mean ± SEM; *P<0.05; **P<0.01; by Mann-Whitney test. n represents numbers of mice. Scale bars: 200 μm (**A**) and 100 μm (**C**).

**Supplemental Figure 13. Decreased LEC TIE2 and p-TIE2 expression in the dorsal skin of E16.5 *Hif2α* LECKO embryos.** (**A**) Representative immunofluorescence staining of TIE2 (green) and LYVE-1 (red) of skin tissues harvested from control or *Hif2α* LECKO E16.5 embryos. DAPI (blue) stains nucleus. White dashed lines demarcate lymphatics. (**B**) Quantification of TIE2 intensity comparing groups shown in **A** (n=5). (**C**) Representative immunofluorescence staining of p-TIE2 (green) and LYVE-1 (red) of skin tissues harvested from

control or *Hif2α* LECKO E16.5 embryos. DAPI (blue) stains nucleus. White dashed lines demarcate lymphatics. (**D**) Quantification of p-TIE2 intensity comparing groups shown in **C** (n=5). Data are presented as mean ± SEM; *P<0.05; **P<0.01; by the Mann-Whitney test. n represents numbers of embryos from 3 litters. Scale bars: 60 μm (**A** and **C**).

**Supplemental Figure 14. Ad*Angpt1*, but not Ad*Angpt2*, treatment effectively alleviates lymphedema in WT mice with lymphatic surgery.** (**A** and **B**) Serial tail volume measurement of mice subjected to lymphatic surgery treated with Ad*Angpt1* (**A**) or Ad*Angpt2* (**B**) (n=4-5). Data are presented as mean ± SEM; ns, not significant; *P<0.05; **P<0.01; by the Mann-Whitney test. n represents numbers of mice.

**Supplemental Figure 15. Sustained LEC HIF-2α expression in the lymphedematous skin of *Hif2α* LECOE mice.** (**A**) Representative immunofluorescence staining of HIF-2α (green) and LYVE-1 (red) of skin tissues harvested from control or *Hif2α* LECOE mice subjected to lymphatic surgery. DAPI (blue) stains nucleus. White dashed lines demarcate enlarged lymphatics. (**B**) Quantification of HIF-2α intensity comparing groups shown in **A** (n=4). Data are presented as mean ± SEM; *P<0.05; by the Mann-Whitney test. n represents numbers of mice. Scale bar: 60 μm (**A**).

**Supplemental Figure 16. Reduced CD45$^+$ cell infiltration in the lymphedematous skin of *Hif2α* LECOE mice.** (**A**) Representative immunofluorescence staining of CD45 (green) of dermal tissue of control or *Hif2α* LECOE mice with lymphatic surgery. DAPI (blue) stains nucleus. (**B**) Quantification of CD45$^+$ cells per field comparing groups shown in **A** (n=5). Data are presented as mean ± SEM; **P<0.01; by the Mann-Whitney test. n represents numbers of mice. Scale bar: 30 μm (**A**).